



**Turbine Design Report – Project Theseus**  
Texas Tech University & South Plains College  
April 18, 2024

Presented By:

<u>Student</u>	<u>Major*</u>	<u>email</u>
Team Leader: Declan Sackett	RE – TTU	<a href="mailto:declan.sackett@ttu.edu">declan.sackett@ttu.edu</a>
Team Co-leader: Nathan Dyer	CE – TTU	<a href="mailto:nathan.dyer@ttu.edu">nathan.dyer@ttu.edu</a>
Prototype Leader: Ethan Avila	EE – TTU	<a href="mailto:ethaavil@ttu.edu">ethaavil@ttu.edu</a>

Prototype Team Members:

David Ellis	IM/ET – SPC	<a href="mailto:dellis1482@southplainscollege.edu">dellis1482@southplainscollege.edu</a>
Iven Ramirez	IM/ET – SPC	<a href="mailto:ivenramirez@southplainscollege.edu">ivenramirez@southplainscollege.edu</a>
Vanessa Romero	IM/ET – SPC	<a href="mailto:vromero0135@southplainscollege.edu">vromero0135@southplainscollege.edu</a>
Mindy Duncan	ME – TTU	<a href="mailto:minddunc@ttu.edu">minddunc@ttu.edu</a>
Jeffrey Fernandez	CE – TTU	<a href="mailto:jefffern@ttu.edu">jefffern@ttu.edu</a>
Reid Jackson	ME – TTU	<a href="mailto:reijacks@ttu.edu">reijacks@ttu.edu</a>

Advisors:

Wheeler Osborne, Instructor, SPC, IM/ET, [wosborne@southplainscollege.edu](mailto:wosborne@southplainscollege.edu)  
Bill Tackett, Instructor, SPC, IM/ET, [btackett@southplainscollege.edu](mailto:btackett@southplainscollege.edu)  
Kacey Marshall, M.A., Assistant Director, TTU Renewable Energy, [kacey.marshall@ttu.edu](mailto:kacey.marshall@ttu.edu)  
Andrew Swift, Sc.D., Professor Emeritus, TTU National Wind Institute, [andy.swift@ttu.edu](mailto:andy.swift@ttu.edu)  
Suhas Pol, Ph.D., Associate Professor of Practice, TTU Renewable Energy, [suhas.pol@ttu.edu](mailto:suhas.pol@ttu.edu)

*\*Abbreviations for listed fields of study:*

*RE – Renewable Energy*

*CE – Civil Engineering*

*EE – Electrical Engineering*

*IM/ET – Industrial Manufacturing/Emerging Technologies*

*ME – Mechanical Engineering*

**TABLE OF CONTENTS**

---

1 Executive Summary ..... 1

2 Technical Design ..... 1

    2.1 Design Objectives ..... 1

    2.2 Continuity from Last Year..... 2

    2.3 Static Performance Analysis ..... 2

    2.4 Mechanical Systems Analysis..... 4

    2.5 Submerged Structure and Anchoring System ..... 6

    2.6 Electrical Systems..... 8

    2.7 Software Architecture ..... 11

    2.8 Team Environment..... 11

    2.9 Commissioning Checklist ..... 12

    2.10 Prototype Laboratory Test Results ..... 12

3 References ..... i

**1 EXECUTIVE SUMMARY**

---

The Techsan Wind Team (TWT) is excited to continue its relationship between the design engineers at Texas Tech University (TTU) & the operation technicians at South Plains College (SPC). This partnership mirrors how industry operates where design and manufacturability must be communicated efficiently while properly addressing problems that may arise during troubleshooting or testing.

This year’s turbine has considerable focus on ease of access to components to support an interchangeable parts philosophy from the powertrain to controls box, and all wiring in between. Inspiration for naming the turbine Project Theseus incorporates this philosophy from the paradox of the ship of Theseus: if all original components of a vessel are replaced, is it still the same object?

The primary objective is to design an offshore wind turbine that can autonomously earn as many points as possible. To maximize scores for turbine performance, the scope of this project closely follows the design objectives for phase 3 turbine performance testing.

**2 TECHNICAL DESIGN**

---

**2.1 Design Objectives**

Initial prototyping is carried out through computer-aided modeling and simulations. This helps to visualize component sizing while providing objects that can easily be numerically evaluated. Most components are bought off the shelf, such as the generator, pitch actuator, yaw servo, yaw sensor, yaw bearing, metal tubing, electrical connectors, resistors, capacitors, microcontrollers, and NEMA enclosures for the controls & load. Some custom parts are required to be

reconstructed from the ground up to support TWT's design philosophy, such as, the nacelle, foundation, and blades.

Region I wind speeds are between 0 and 4.9 m/s. Blades will be pitched to achieve the lowest cut-in speed. During this phase, the turbine is still pulling power from the DC power supply and steadily increasing in rpms. Region II wind speeds are between 5 and 11 m/s, at 5.5m/s a relay will cut off the DC power supply and divert the three-phase power to the load resistor. At this point the turbine's electrical components will run off the turbine's generated power and the blades will pitch to the run angle to maximize power production. Region III wind speeds are between 12 and 22 m/s. The turbine will actively control the pitch angle of the blades to maintain produced power and rotor speed at the rated wind speed of 11 m/s. Region IV wind speeds are above 22 m/s and are not expected to be produced by either the TWT or CWC wind tunnels.

An emphasis on safety is imperative, as failure to comply poses risks of injury but also jeopardizes eligibility for future competitions. To prevent runaway situations, the turbine autonomously detects load disconnection, stopping rotation until reconnection with the simulated grid prompts power generation to resume. The manual emergency stop procedure ensures the turbine's complete shutdown upon command. Similarly, the turbine will resume power production once the emergency stop signal has been reset.

Power will be produced for the entirety of the test for wind speeds up to 22 m/s with the load engaged while adjusting pitch according to varying wind speeds. Theseus' foundation, which consists of an auger system, will hold the turbine upright up to 20 m/s.

## ***2.2 Continuity from Last Year***

Yaw bearing – a 1.5 in. inner diameter flange bearing helps maintain aesthetics by providing a uniform appearance among transition piece and tower.

Pitch motor – this linear actuator has consistent performance and reliable position accuracy.

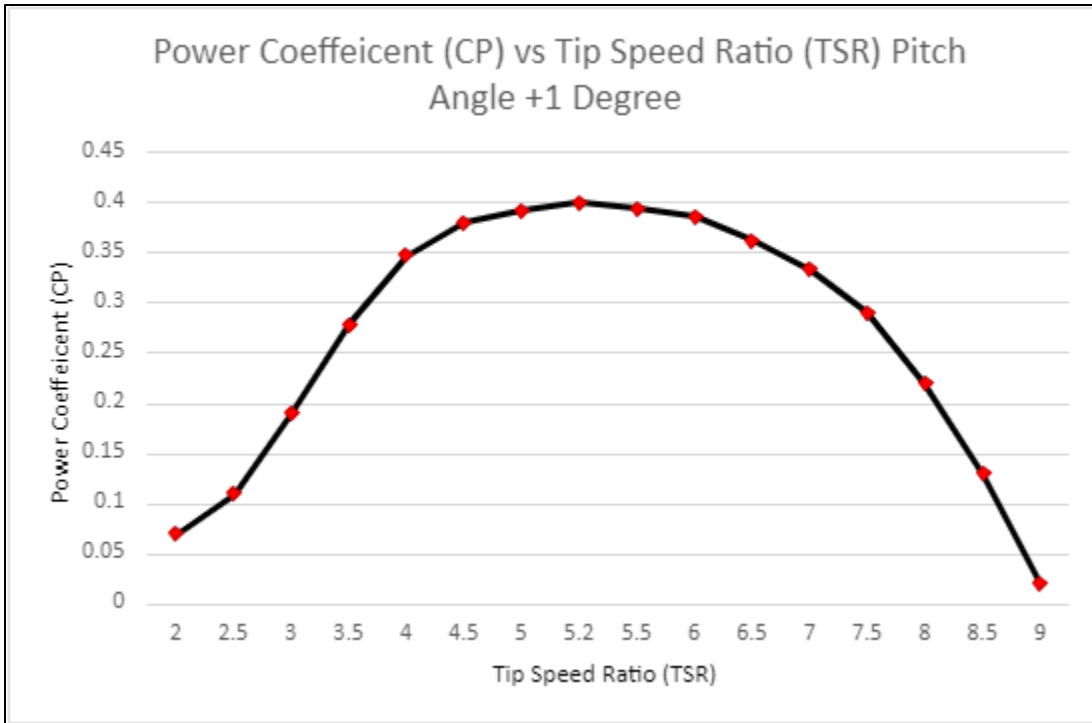
R/C helicopter rotor hub – the compact design has a shaft that allows the blades to connect directly to the generator with a swash plate that manipulates pitch.

A/C generator – this generator has been proven in previous years to reliably produce power up to, but not exceeding, the maximum 48 V requirement at a low amperage which minimizes electrical losses.

Controls hardware components – limited to: 7.2  $\Omega$  load resistor, buck-boost converters, relays, Arduino Uno. The resistor provides the most power at rated wind speeds for our selected generator; constructing buck-boost converters that can accurately control and display voltage was not deemed to be within the scope of the project for TWT; similarly, with relays, designing & constructing novel relays is not within the scope of the project for TWT; Arduino Unos provide sufficient microcontroller capacity for TWT to compile innovative processes each year. Blades – the same airfoil profile is being used but has been manufactured from carbon fiber.

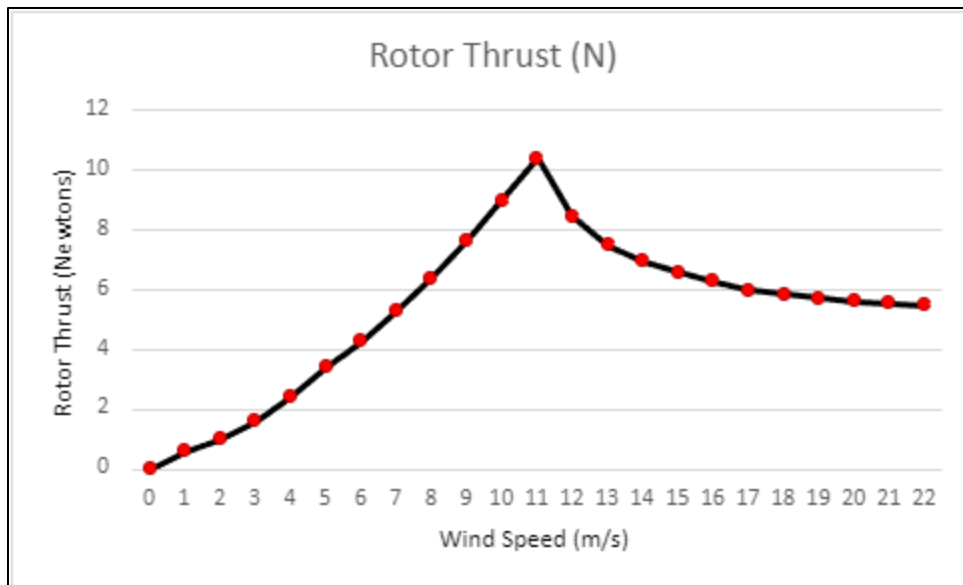
## ***2.3 Static Performance Analysis***

For the rotor performance analysis, QBlade software was used. Using the Davis 3R airfoil, Figure 1 shows the Power Coefficient - Tip Speed Ratio (TSR) for a pitch angle of +1°, with a maximum power coefficient ( $C_p$ ) of 0.4 at a TSR of 5.2.



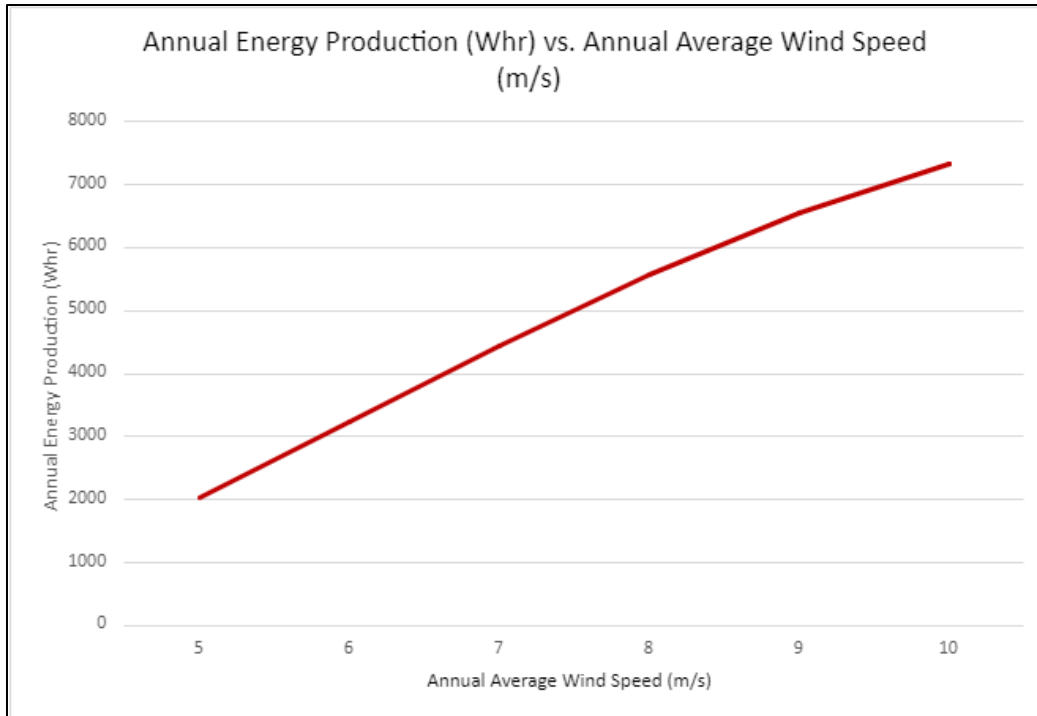
**Figure 1: Power Coefficient vs Tip Speed Ratio results using QBlade Software**

Figure 2 shows the QBlade predicted rotor thrust (N) with a maximum thrust of 12 N at a wind speed of 11 m/s.



**Figure 2: Prototype QBlade Predicted Operational Thrust Data.**

Figure 3 shows the calculated annual energy production with a maximum value of 7,337 Whr at an annual average wind speed of 10 m/s.



**Figure 3: Calculated Annual Energy Production assuming a Rayleigh Wind Speed Distribution.**

### 2.3.1 Experimental Set-Up

A wind tunnel similar to the CWC small wind tunnel was used for the testing, which includes an interface compatible with offshore foundation testing. The tunnel is equipped with a pitot-static tube for measuring wind speed and instruments to monitor temperature, pressure, and humidity. Additional equipment includes a laser tachometer, devices for measuring resistive load, voltage, and current, and an external power supply.

### 2.3.2 Annual Energy Production

The maximum possible energy output would occur if the wind speed at the location of the turbine were always greater than or equal to 10 m/s and below 21 m/s. At these speeds Theseus generates at rated power, 25 W, over a year this would equal 219 kWh/yr. Using 40 years of hourly wind speed data at 50 m over Lake Michigan from the MERRA 2 aggregate meteorological model, a Weibull distribution was created to model Theseus’ performance. Using our measured power values for each wind speed from 0-21 m/s, an annual energy production of 127 kWh/yr is estimated, a capacity factor of 58%.

## 2.4 Mechanical Systems Analysis

The blades incorporate two outer carbon fiber sheets with a carbon spar, a Smooth Cast 300 root, and a final silicon resin coating. The blades use a Davis 3R airfoil, with the same twist and taper as last year shown in Figure 4. The continued use of Davis 3R airfoil is supported by its performance at low Reynolds numbers. The carbon fiber reduced the blade weight from 25.3 g to 12.8 g and the cost of production by a factor of 10, compared to the aluminum blades used last year. The carbon fiber blades were modeled in QBlade and were made in-house by our team members at SPC. The blades were manufactured using a multi-step process. The first step

involved molding the carbon fiber blade. Next, the blade was coated with silicon resin by a second molding process. Finally, a third molding process was used to create the blade root.



Figure 4: Blade comparison

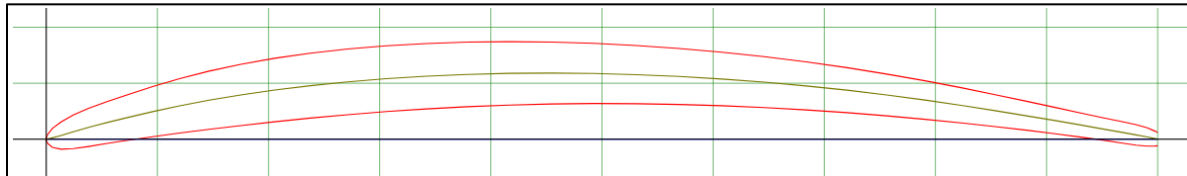


Figure 5: Davis 3R Airfoil Profile

The nacelle subsystem assembly, shown in **Error! Reference source not found.**, is comprised of two 3D-printed major components: a frame and detachable aerodynamic body panels. The frame provides a structure to mount powertrain components, electrical components, wire terminations, and body panels. The nacelle was designed to avoid the potential of wires becoming entangled on the rotating shaft or ensnared in the yaw gears. Experience from previous years has demonstrated the need for ease of access to all components without requiring completely disassembling the turbine. Therefore, electrical components, motors for pitch & yaw, yaw position sensors, and the generator have been placed such that there is enough clearance for the wiring harness, and serviceability should any component need replacing. Locations for electrical terminations were selected to guide wires from the wiring harness and electrical components away from hazardous points of contact. The ends of wires are terminated with o-type terminal connectors. Continuity is established by overlapping similar terminals, then securing the pair to the frame with a screw through the holes. Body panels resemble a truncated prolate spheroid which is commonly used in sports, like rugby and American football, where aerodynamic shapes are necessary to combat air resistance. Once the nacelle has been fully wired and mounted to the tower, the body panels are then attached to enclose the subsystem.

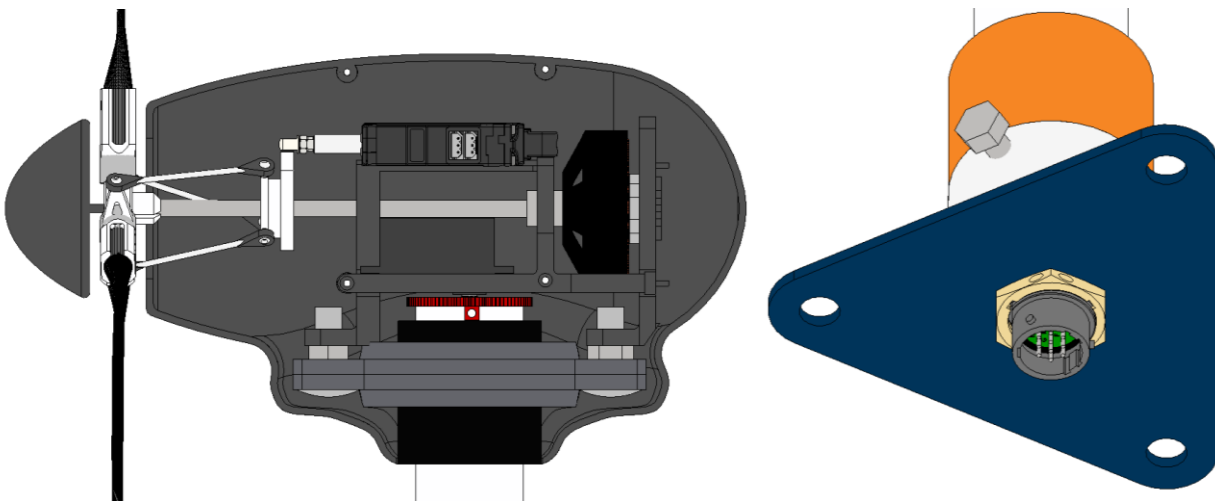


Figure 6: Turbine Nacelle and Base

A hollow aluminum tower, shown in Figure 6, connects the nacelle to the provided transition piece and encases the internal wiring harness. Atop the tower is a 2-bolt flange bearing to provide mounting posts for the nacelle and yaw capabilities. Magnets placed on the top of the tower within the nacelle are detected by yaw position sensors that designate critical points for normal operation and E-stop procedures. The base of the tower is an iron pipe larger than the tower welded to an iron triangle with bolt patterns to match the transition piece and a hole for a 10-pin bayonet electrical connector to pass through. The aluminum tower is held in place by three set screws integrated into the iron tower base pipe.

#### **2.4.1 Expected mechanical loads**

The wind will create thrust in specific areas of the mechanical systems, primarily due to drag. Blades will generate 12 N of thrust at 11 m/s, as they rotate through the rotor, and the nacelle will exert force similar to the blades, positioned at the same height as the rotor. Additionally, the tower will experience thrust concentrated at its midpoint.

#### **2.4.2 Safety factors**

The most readily compromised mechanical system are the three blades. This is due to centripetal forces at the point of contact for the screw that secures the blades into the blade housing during runaway conditions and bending with blades flat against the rotor thrust. Assuming simplifications, such as a rectangular blade cross-section and uniform silicon resin material, the estimated yield strength at a wind speed of 22 m/s and +3,000 RPM was found to be 4.22 MPa and with an allowable yield strength of 36 MPa, the blades have a Factor of Safety (FoS) of 25.35 for each blade during runaway conditions. Additionally, there is a FoS of 63.68 for blades bending during parked conditions after stopping for load disconnect at 14 m/s.

### **2.5 Submerged Structure and Anchoring System**

The turbine prototype's foundation, shown in Figure 7, consists of a steel baseplate anchored by two auger piles windward and is supported by a circular footing in the rear. This circular footing is the core of the baseplate and features a diameter of 15.2 cm. From it extends two arms of width 3.8 cm, protruding away from and in front of the circular center, each at a 45° angle from the centerline. These arms each house an auger at the end, ensuring the anchor support is as far away as possible from the center to provide optimum leverage. The augers are just shy of the bore depth limit, at 19.5 cm in length, to maximize stability provided by the soil at depth. These protect the foundation from an overturning moment. The remainder of support for the foundation is supplied by the circular baseplate, which utilizes the bearing capacity of the soil to prevent tipping from an overturning moment.

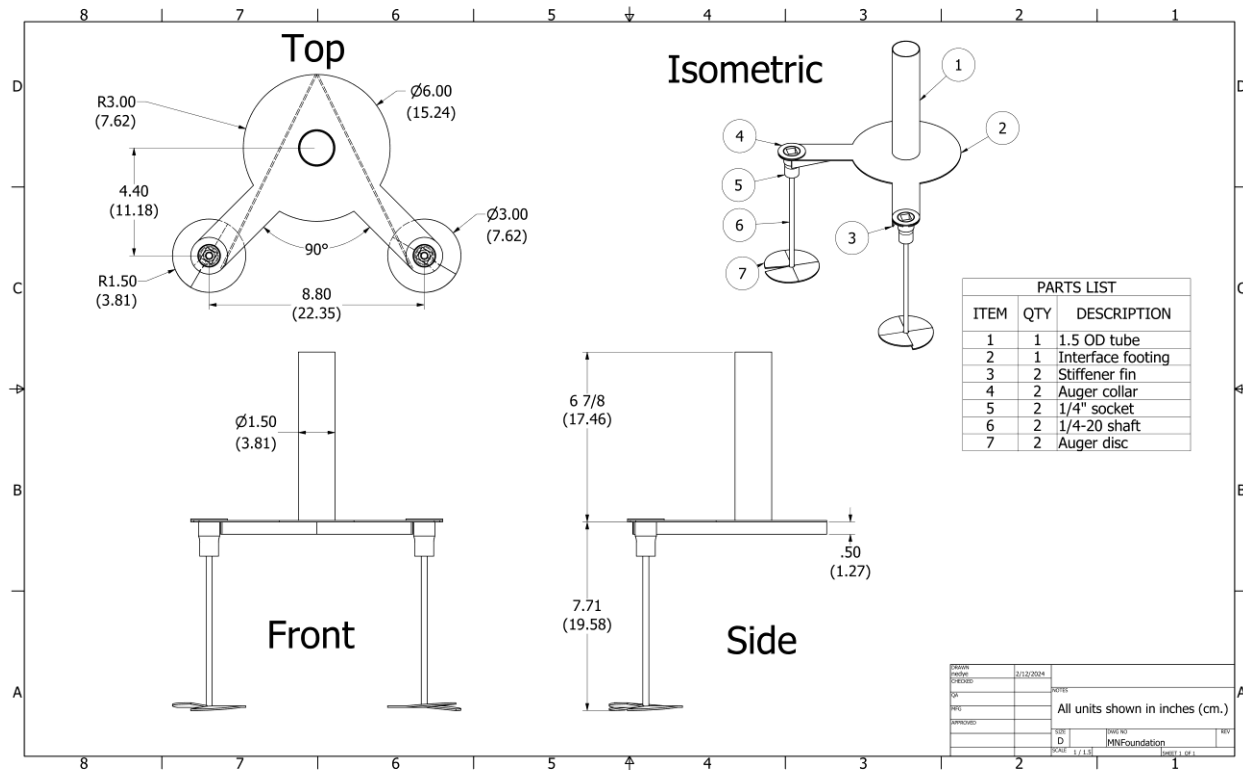


Figure 7: Structural Foundation (3<sup>rd</sup> Angle Projection)

### 2.5.1 Foundation

The foundation is a flat steel plate, 2 mm thick, connecting to the tower at the center of a circular footing, which has a diameter of 15.2 cm. Extending from this footing, each at a 45° angle, are arms that house augers at their ends. These arms are each 3.8 cm wide and reach into the corners of the Offshore Simulation Box, to allow the augers to achieve maximum leverage.

### 2.5.2 Anchoring system

The anchoring system of the baseplate is two auger piles positioned on the windward side. Each auger, when tested, supplied 133.3 N of resistance, which comes from both the pressure acting on the auger disc itself and the friction force experienced by the shaft interacting with the soil. The auger piles themselves are 19.5 cm long, with the auger disc being 3.81 cm in radius, and the top plate with a radius of 4.45 cm.

### 2.5.3 Structural analysis

At the maximum thrust produced during the test, occurring at 11 m/s, the nacelle and blades are expected to produce 14.3 N of thrust. This force, being applied 0.60 m above the baseplate results in an overturning moment of 8.6 N·m about the core of the baseplate, where the tower meets the plate. To prevent tipping, the sum of resisting moments must match or exceed that value. The auger piles together have been tested to return a resisting moment of 29.8 N·m. Now, the circular footplate with a diameter of 15.2 cm utilizes the bearing capacity of the sand, at

140,000 N/m<sup>2</sup>, to support a force of up to 2,520 N, therefore having a calculated resisting moment of 47.2 N·m. The summation of the moments about the center of the baseplate;

$$\Sigma M = -8.6 + 29.8 + 47.2 = 68.5 \text{ N}\cdot\text{m}$$

Therefore, the foundation should be secure from an overturning moment, and comfortably exceed our Factor of Safety of 4.

### 2.6 Electrical Systems

The generator is a T-Motor antigravity MN5008 3-phase drone motor operating as the turbine’s generator. The motor has low cogging torque and is ultralight with a motor efficiency of 75% and an estimated generator efficiency of 50%. The stator is an imported silicone steel sheet, with antirust treatment rated for up to 180°C operation. The shaft diameter is 6 mm with imported 696ZZ bearings. The coil insulation is rated for 500 V with a centrifugal cooling design. The generator size is 55.6 mm in diameter by 32 mm thick and weighs 128 grams. The motor/generator is rated for 47 V, 11.5 A, and 6,300 RPM.

A system one-line diagram is shown in Figure 8, canonical model in Figure 9, and 10-pin schematic in Figure 10 below.

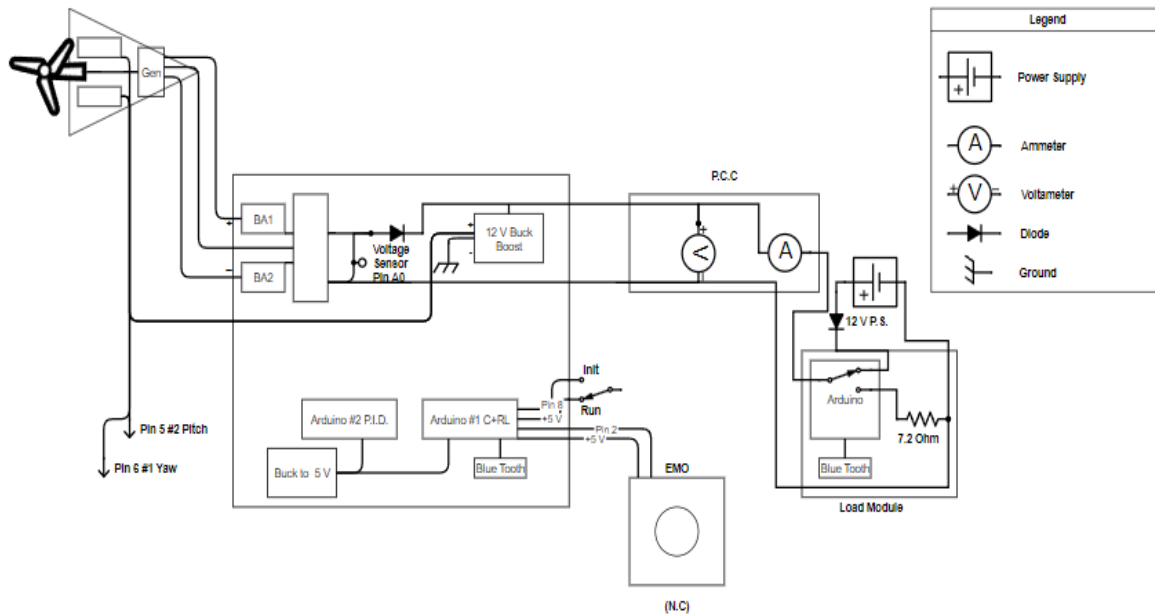


**Figure 8: Control System One-Line Diagram**

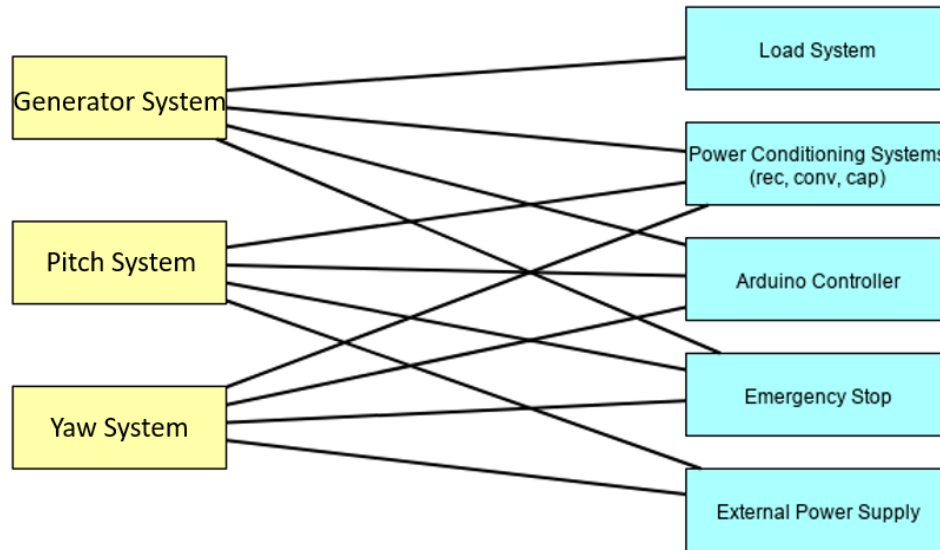
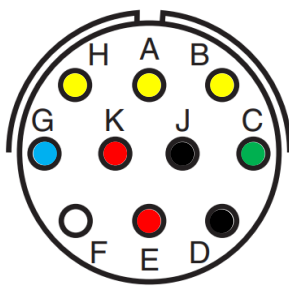


**Figure 9: Canonical model**



A	18 AWG A/C
B	18 AWG A/C
C	22 AWG yaw signal
D	22 AWG reed relay supply
E	22 AWG reed relay ground
F	22 AWG not used
G	22 AWG pitch signal
H	18 AWG A/C
J	18 AWG VDC negative & earth ground
K	22 AWG VDC positive

**Figure 10: 10-pin wiring layout**

The control box uses two Arduino microcontrollers to host code for the autonomous features of the turbine. The Arduino reads the external initialize switch as an input to enter the initialize or start phase of the test. The team used an external DC power supply set to 12 V and this power is split with one path going through pin K of the 10-pin connector to the servo’s positive terminals and a buck-boost converter which steps the 12 V down to 6 V to power the Arduinos. For blade pitch control, the team used a discontinuous linear actuator that uses Pulse Width Modulation (PWM) signals from the Arduino’s output pins to manipulate pitch to precise angles. The yaw servo is continuous and uses a reed relay as a flag at the 90° yaw angle. This ensures consistent yaw control in and out of the wind for the turbine despite installation alignment.

When the turbine begins generating sufficient power, the three-phase power from the generator is fed back to the control box through pins H, A, and B of the 10-pin connector. They then go through a rectifier to convert AC to DC power then a 2,000 μF capacitor to smooth the voltage output for the Arduino A0 pin to read. This power is also fed to the load box which contains a 7.2 Ω resistor that is rated for 150 W. At this point in the test, the power generated by the turbine is used as a substitute for the DC power supply as a relay closes off this source and the turbine begins operating off its own generated power. Some generated power is stepped down to 12 V

and sent down the same path as the DC power supply for the servo’s and Arduino’s positive terminals.

When the E-stop button is pressed, the turbine enters an emergency stop procedure where the Arduino relay shorts the three-phase power from the generator to stop it. The main Arduino then pitches the blades to a stall angle and yaws the turbine out of the wind, ensuring a complete stop. The turbine will remain in the E-stop position until the button is lifted. When this happens, the servo will yaw the turbine back into the wind, pitch the blades to the start angle, and then disengage the Arduino relay returning the turbine back to its standard operating mode. During the load disconnect phase of the test, the team needed a way to detect when the load was disconnected and a way to power the turbine until the load was reconnected. The team built a custom Power Control Hub (PCH) hosted in the control box to monitor power and voltage generated. When the load is disconnected, the voltage will spike and power will drop to zero which the main Arduino will detect and begin the emergency stop procedure without the need to push the E-stop button. Due to limited power when the load is disconnected, the Arduino relay will only short one phase from the generator and pitch the blades to the stall angle. The turbine will not yaw out of wind during this phase of the test but a complete stop will still happen. When the load is re-connected, the blades will pitch back to the start angle and the Arduino relay will be deactivated. The pitch will then shift to the run angle thus restarting the turbine.

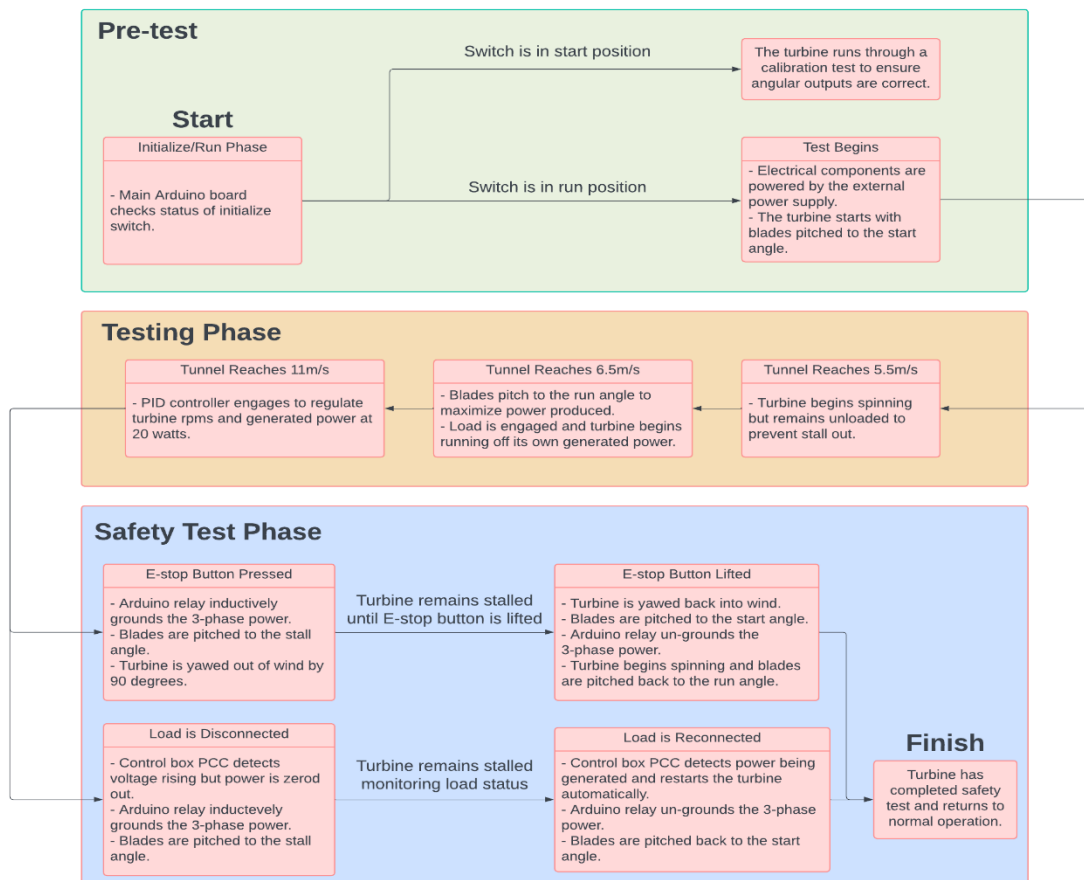


Figure 11: Turbine Control Sequence

## ***2.7 Software Architecture***

The team utilized multiple Arduino boards communicating via Bluetooth to host all autonomous features of the turbine. The Arduino Integrated Development Environment (IDE) allows for loops that repeatedly run code during the test. This allows for a dynamic system that ensures the conditions for the various states of the code are checked continuously. The main Arduino board has a pin connected to the initialize switch for a pre-test calibration feature to ensure both the blades and turbine move to their respective pitch and yaw angles during the test. The team implemented this safety feature to ensure that all components are operating as expected before the test begins. There were also issues last year with the yaw servo requiring different PWM signals based on installation alignment. To fix this, the team converted the servo to operate continuously and use an external reed relay as a flag in the nacelle. This allows the main Arduino to output a PWM rotational signal to yaw the turbine from its start position until it reaches its flag at 90° yaw. This ensures that no matter the alignment of the turbine, it will always yaw into and out of the wind correctly. When the initialize switch is in run mode, the turbine remains idle, reading the rectified DC voltage through the A0 pin. This voltage acts as our conditional statement for the main portions of the test.

When the A0 pin reaches a specified Arduino count, the pitch actuator receives a new PWM signal to pitch the blades to the run angle. The main Arduino will then send a signal via Bluetooth to the load box Arduino which will engage a relay to begin generating power. When this happens, the turbine begins running off its own generated power. The team had issues in the past with the turbine rotor stalling out due to the blades being unable to revert to the start pitch angle if the A0 value fell back below the specified count. The team has since then improved the robustness of the code to account for this by allowing the turbine to revert back to the start angle. When the wind tunnel reaches 11 m/s, the turbine regulates the 20 W generated by using a coded Proportional Integral Derivative (PID) Controller hosted in the PID Arduino board. This controller takes the error from the desired A0 and current A0 counts. It then calculates a corrective output to the pitch PWM signal to pitch the blades into and out of the wind to regulate RPM and generated power.

The PID Arduino board also contains the Emergency stop procedure and constantly checks the button's output to ensure a quick stop when pressed. When this button is pressed, the Arduino sends a signal to the Arduino relay to short the 3-phase output of the generator. It then sends new PWM signals to the pitch and yaw servos to pitch the blades to the stall angle and yaw the turbine out of the wind by 90°. This ensures a complete stop under the 10-second requirement and meets the safety requirements of this portion of the test. When the button is lifted, this process is repeated in reverse to restart the turbine back to normal operation. During the load disconnect phase of the test, the main Arduino will monitor the power generated via the control box's PCH. When the load is disconnected, the power will drop to zero but the voltage will spike. The main Arduino detects this and begins the load disconnect phase.

## ***2.8 Team Environment***

The team functions as a partnership between SPC consisting of student technicians and TTU consisting of engineering students. To parallel a real-world working environment, the team operates with TTU managing design choices and reports and SPC managing manufacturing and assembly. Every student has a choice on what component of the turbine they focus on related to

their desired career paths. This creates a team environment where everyone can show how their specialty contributes to the final product. Due to the distance between the two campuses, the teams meet weekly at the Reese Technology Center, located between the campuses.

**2.9 Commissioning Checklist**

<b>Pre-installation:</b>	<b>Performed by:</b>	<b>Verified by:</b>
Assemble the nacelle and tower.	VR	EA
Perform continuity tests on all electrical components including all 10-pin connector pins.	VR	EA
Attach body panels to the nacelle.	DE	ND

<b>Foundation Install:</b>	<b>Performed by:</b>	<b>Verified by:</b>
Feed wiring harness through the foundation	VR	JF
Three students will head to the tunnel early on standby until our timeslot to install the foundation.	ND/JF/DE	EA
Two students will drill the augers in while the third ensures connections remain dry.	ND/JF/DE	ND

<b>Turbine Install:</b>	<b>Performed by:</b>	<b>Verified by:</b>
Three students will walk to the table with the control box, load box, and power supply.	VR/IR/EA	DS
A fourth student follows with tools in case of emergency.	MD	DS
One student will be tasked with ensuring the E-stop button is lifted and connect it to the control box.	VR	EA
One student will connect Theseus to the PCC	IR	EA
Foundation is wheeled in and 10-pin connector is fed through the tunnel.	DE	ND
A student will bring the turbine to the tunnel to be installed and will connect the 10-pin to the turbine.	RJ	DS
Once the turbine has been installed and all electrical connections have been made, the team will run through a final check to ensure everything is in working order	VR/IR/DE	EA/ND

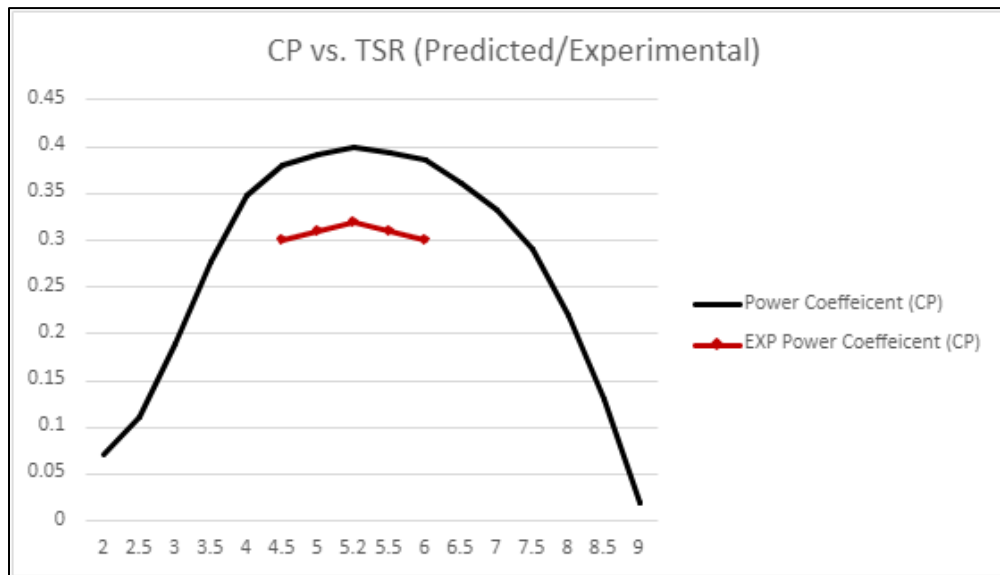
**2.10 Prototype Laboratory Test Results**

The prototype turbine performance was measured using the wind tunnel as described in the Experimental Set-Up. A reasonable agreement was observed between experimental and analytical data. The solid red line in Figure 12 shows the QBlade generated power vs. wind speed for the model turbine. The power increases proportionally to the wind speed cubed (Region II) and is constant beyond the rated wind speed (Region III). The experimental measurements align closely with the QBlade-generated power curve. The differences can be likely attributed to the limitations of the generator, which is a drone motor. This can be clearly observed in the differences between the predicted and the measured rotor speed at higher wind speeds. Further, the pitching schedule for the maximum possible  $C_p$  at different wind speeds is

**Table 1: Experimental Data from laboratory setting**

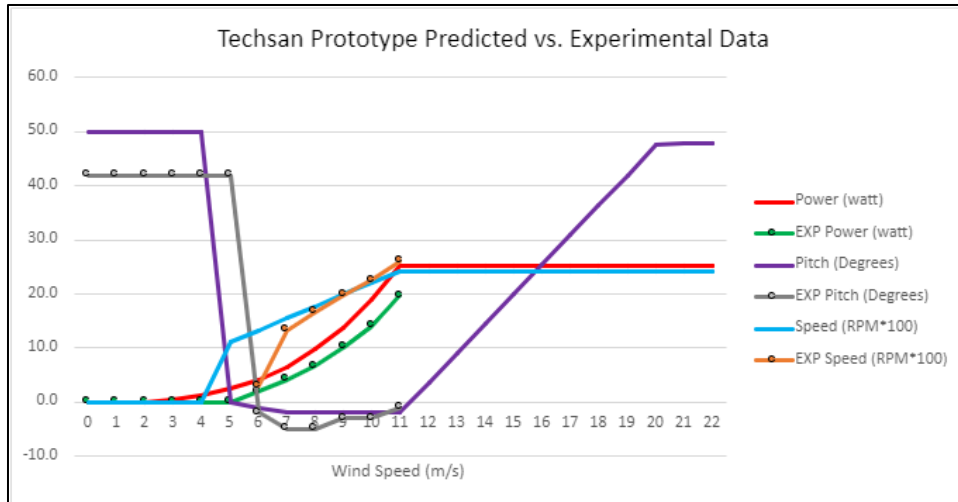
Test Data Inputs			calculated values									
temp	deg F>	70	deg C>	21	<b>Prototype test, Reese Technology Center, 1018 m. sta elevation</b> date: 4/11/2024 time: 6pm							
Bar Press	inches Hg>	30.01	mb>	1016								
Humidity	%>	50										
Gen. Load	Ohms>	7.2										
Yaw Angle	degrees>	0										
	Station	Pressure>	inches Hg>	26.56	mb>	899						
	Dry	air density>	kg/m^3>	1.07								
	Moist	air density>	kg/m^3>	1.2	<a href="#">Click here</a> ...calc moist air density; Using Omnicalculator/physics/airdensity							
Operational Data inputs												
Red Oil	Electronic											
Pitot Tube meas.	Calculated wind speed	Testo wind speed	Arduino pitch angle	Blade pitch angle	RPM	Gen volts	Gen amps	Gen watts	Load in Ohms	Average Wind Speed	TSR	
Inches H2O	m/s	m/s	dim	deg	rev/min	volts	amps	watts	Load in Ohms	Average Wind Speed	TSR	
0.08	5.77	6.2	93	-1	300	3.75	0.524	1.965	7.2	5.99	0.9	
0.11	6.77	7.1	94	-2	1330	5.5	0.763	4.1965	7.2	6.94	3.3	
0.14	7.64	8.1	94	-2	1664	6.89	0.9557	6.584773	7.2	7.87	3.7	
0.18	8.66	9	94	-2	1980	8.502	1.196	10.168392	7.2	8.83	3.9	
0.24	10.00	10	94	-2	2248	10.06	1.393	14.01358	7.2	10.00	3.9	
0.28	10.80	11	94	-2	2605	11.913	1.642	19.561146	7.2	10.90	4.2	

shown in Figure 13 as well. Since the experiments were conducted in Region II, the operating pitch was changed based on QBlade-derived optimal pitch values, however the actual pitch values varied slightly. Furthermore, measured vs. QBlade predicted  $C_p$  vs. TSR is shown below in Figure 12. The model TSR ranged between 4.5 and 6 for various inflow wind speeds as tabulated in Table 1 above. The measured  $C_p$  ranged from 0.3 to 0.32 for turbine operation in Region II. The 50% generator efficiency was accounted for in this measurement. This performance data again demonstrates the agreement between experimental values and QBlade predicted values.



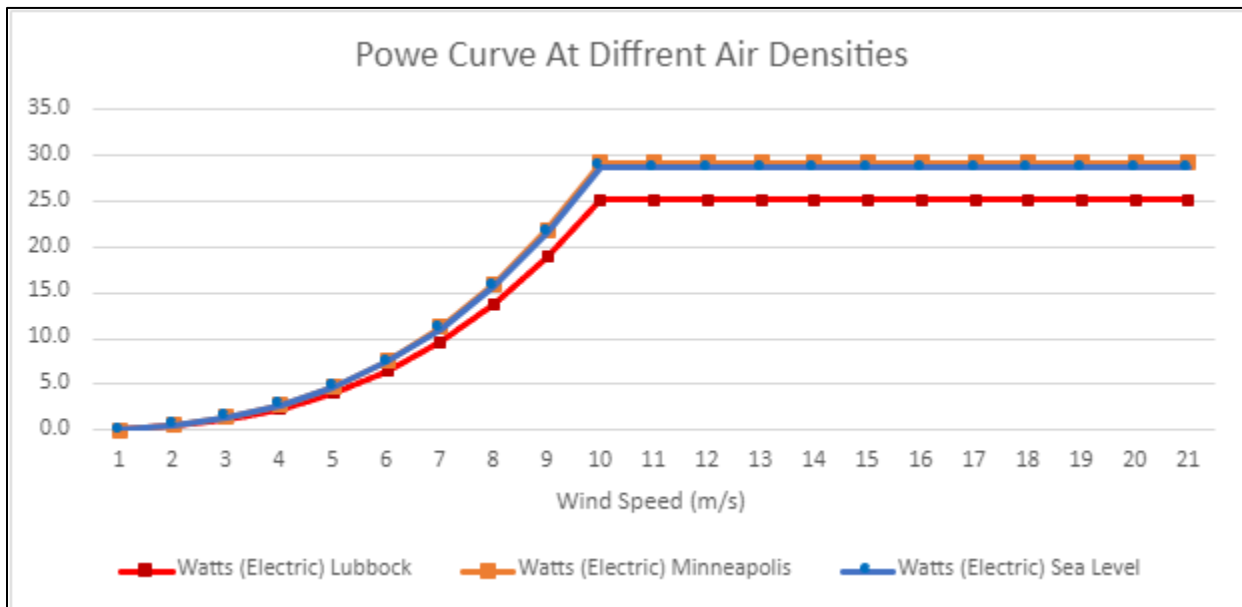
**Figure 12: Measured vs. QBlade predicted  $C_p$  vs. TSR.**

The test data above was then used to generate the prototype power curve and compared with the QBlade predictions. Figure 13 shows the comparison with a Variable Data Chart which includes pitch angle, output power in Watts (Electric), and  $RPM \times 100$ . The solid lines show the QBlade predictions for each variable while the dots show experimental results from wind tunnel tests.



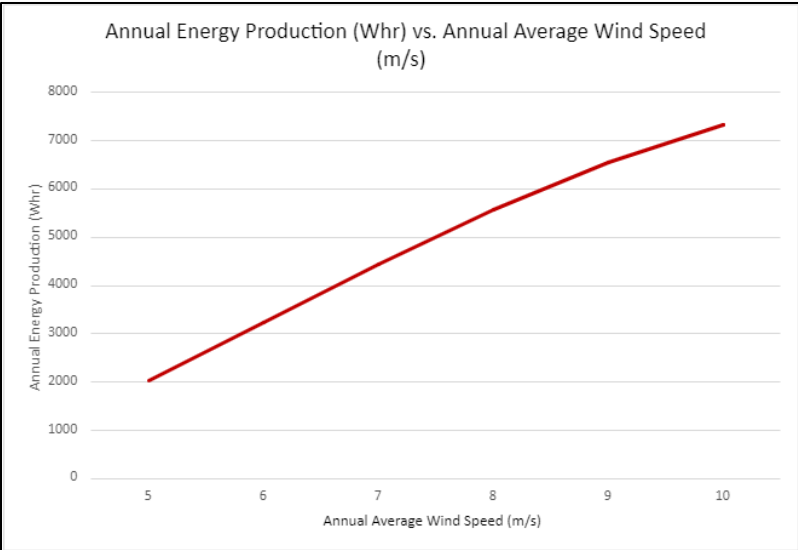
**Figure 13: Prototype QBlade Code and Experimental Wind Tunnel Data.**

Figure 14 shows expected power curves set at different air densities including sea level (1.23 kg/m<sup>3</sup>) with a rated power of 28.7 W, Lubbock, Texas (1.04 kg/m<sup>3</sup>) at 25.2 W, and Minneapolis, Minnesota (1.0 kg/m<sup>3</sup>) at 29.2 W.



**Figure 14: Expected Prototype Power Curves for various locations.**

Figure 15 shows the calculated Annual Energy Production, which was calculated using the power curves in Figure 14.



**Figure 15: Annual Energy Production vs. Annual Average Wind Speed**

### 3 REFERENCES

---

Hansen, Martin O.L. “Aerodynamics of Wind Turbines”, Routledge, ISBN 9781138775077, 113877507X, 2015

Swift, A., “Rotor Aerodynamic Modeling using Blade Element Momentum (BEM) Methods”, Texas Tech University, National Wind Institute, Internal Document, 2011

MN5008 KV170. T-motor. Retrieved April 18, 2024, from <https://store.tmotor.com/product/mn5008-kv170-motor-antigravity-type.html>

299:LP. Reefs, Retrieved April 18, 2024, from <https://reefsrc.com/products/299-lp-racing-servo>

12LF-20PT-27. MightyZAP. Retrieved April 18, 2024, from <https://www.digikey.com/en/products/detail/mightyzap/12LF-20PT-27/13681490>

PT06E-12-10S(470). Amphenol Industrial Operations. Retrieved April 18, 2024, from <https://www.digikey.com/en/products/detail/amphenol-industrial-operations/PT06E-12-10S-470/1209852>

PT07A12-10P-025. Amphenol Industrial Operations. Retrieved April 18, 2024, from <https://www.peigenesis.com/en/shop/part-information/PT07A1210P025/APH/EACH/4532212.html>

Army Corps of Engineers, “Bearing Capacity of Soils”, American Society of Civil Engineers, ISBN 9780872629974, 087262997X, 1993

[Airfoil Tools. \(n.d.\). http://airfoiltools.com/airfoil/details?airfoil=davissm-il](http://airfoiltools.com/airfoil/details?airfoil=davissm-il)